Appl. Phys. B 87, 207–210 (2007)
DOI: 10.1007/s00340-007-2601-2

Applied Physics B
Lasers and Optics

F. THÉBERGE[1,✉]
J. FILION[1]
N. AKÖZBEK[2]
Y. CHEN[1]
A. BECKER[3]
S.L. CHIN[1]

Self-stabilization of third-harmonic pulse during two-color filamentation in gases

[1] Centre d'Optique, Photonique et Laser (COPL) and Département de Physique, de Génie Physique et d'Optique, Université Laval, Québec, Québec G1K 7P4, Canada
[2] Time Domain Corporation, Cummings Research Park, 7057 Old Madison Pike, Suite 250, Huntsville, AL 35806, USA
[3] Max-Planck-Institut für Physik komplexer Systeme, Nöthnitzer Str. 38, 01187 Dresden, Germany

Received: 20 November 2006/Revised version: 29 January 2007
Published online: 24 March 2007 •

ABSTRACT Self-stabilization of the laser pulse parameters is demonstrated during the two-color filamentation of ultrashort and intense laser pulses in gases. Experimental data and results of numerical simulations show, in good qualitative agreement, that the root-mean-square values of the intensity fluctuations decrease below the initial value for the near-infrared pump pulse and the perturbative limit for the third-harmonic pulse in the filament. It is found that the stabilization of the third-harmonic intensity and energy are due to intensity clamping of the pump pulse and a constant 'volume' of the laser pulse during the nonlinear propagation inside the filament.

PACS 42.65.Ky; 42.65.Jx; 52.35.Mw

1 Introduction

Nowadays, intense ultrashort laser pulses are a basic tool in many branches of physics and chemistry [1, 2]. Recently, it was demonstrated that filamentation of infrared femtosecond laser in gases leads to a self-compression [3] of the pulse to a few cycles, potentially even to the single-cycle limit [4]. Remarkably, the self-compressed pulse preserves a stable carrier-envelope offset phase during the filamentation [3, 5]. The non-linear propagation of ultrashort laser pulses in optical media is mainly governed by the dynamic interplay between the optical Kerr effect due to the intensity-dependent refractive index and defocusing from a low-density plasma induced by multiphoton/tunnel ionization (for recent reviews see [6]). The defocusing effect of the self-generated plasma balances the self-focusing effect and leads to a limited peak intensity of about 5×10^{13} W/cm^2 during the laser pulse propagation in air [7]. This is known as intensity clamping [8, 9] and results in the stabilization of the pump intensity inside the filament [10]. Moreover, it has been shown that the intensity inside the filament is sufficiently high to induce third-harmonic generation [11]. Indeed, it has been shown theoretically that the fundamental and the third-harmonic pulses are coupled inside the filament due to a nonlinear group-phase-locking effect [11]. Results of subsequent numerical simulations [12] suggested in addition that the axial component of the third-harmonic radiation can be compared to a forced oscillator driven by the fundamental, while the rings of the third harmonic appear due to phase matching over a longer propagation distance. The mechanism of self-group-phase locking also holds for other parametric processes such as four-wave mixing [10], and fifth harmonic generation [13].

The self-actions during the filamentation are crucial for several applications based upon the generation of few-cycle pulses [3] and high-harmonics [14] through the filamentation in gases. In this work, we verify the self-stabilization of the laser pulse parameters during two-color filamentation. Our study shows that the pump intensity, the third-harmonic intensity and the energy of the third-harmonic pulse are stabilized during filamentation. Surprisingly, the self-stabilization of these laser parameters was not accompanied by a stabilization of the pulse duration.

✉ Fax.: 1-418-656-2623, E-mail: francis.theberge.1@ulaval.ca

2 Experimental setup

Depending on the particular nonlinear interaction inside the filament, it is sometimes not trivial to measure the signal inside the core of the filament without destroying partially its excellent parameters. For example, the third-harmonic (TH) generated inside the two-color filament [11] destructively interferes with the TH generated after the filament. This is the result of the Guoy phase shift in which the TH energy generated in the filament is given back to the pump after the geometrical focus [15]. The linear wave-vector mismatch between the pump and the third-harmonic is large and thus the distance to decouple the fundamental and the third-harmonic laser pulses beyond the filament is critical for the measurement of the TH energy stability inside the filament. The experiment was done by using an energy per pulse of 680 μJ (2 times the critical power for self-focusing in air) and a transform limited pulse duration of 40 fs at full width at half maximum (FWHM). The radius of the elliptical beam mode at the $1/e^2$ level was $r_H = 3.4$ mm and $r_V = 2.3$ mm where r_H and r_V are horizontal and vertical radius, respectively.

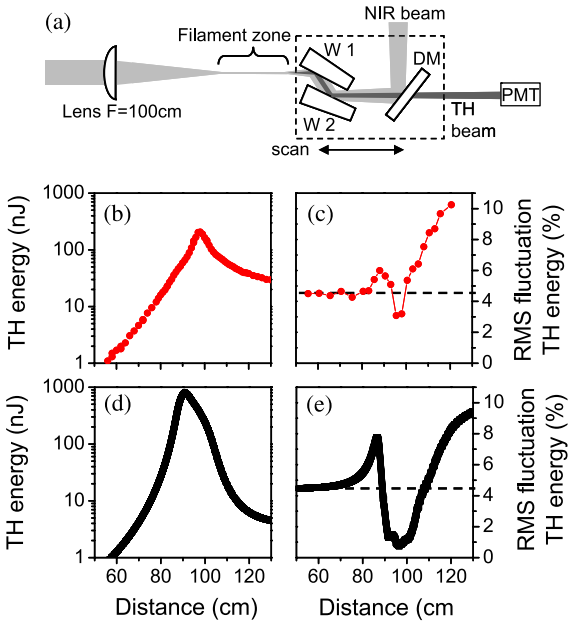

FIGURE 1 (**a**) Experimental setup to measure the third-harmonic energy along the propagation axis. (**b**) Experimental results of the third-harmonic mean energies as a function of the propagation distance and (**c**) the corresponding RMS energy fluctuations. (**d**) Numerical simulations of the third-harmonic mean energies as a function of the propagation distance and (**e**) the RMS energy fluctuations

The pulse was focused into air at ambient pressure using a 100 cm focal length lens to generate single plasma column of about 5 cm long. The plasma column starts around 95 cm and ended at 100 cm. Since the laser intensity inside the filament core is above the damage threshold of the decoupling mirror (see DM in Fig. 1a), the surface reflections from a pair of wedges (W1, W2) set at large incidence angles were used to decrease the intensity of the laser pulses on the surface and thereafter the dichroic mirror (DM) was used to suppress the near-infrared (NIR) laser pulse and transmit the TH beam as shown in Fig. 1a. This experimental setup was scanned along the propagation axis and could cease the filamentation process if the first wedge (W1) was positioned inside the filament zone. The TH pulse energy was measured with a calibrated photomultiplier tube.

3 Experimental results

Figure 1b shows the measured third-harmonic mean energy along the propagation axis. The TH energy is roughly constant inside the filament zone between 95 cm to 100 cm. Beyond the filament, the destructive interference induced a decrease of the TH energy and become constant around 130 cm due to a spatial walk-off between the NIR and TH pulses. The root-mean-square (RMS) intensity fluctuation of the input NIR pulses was 1.5% in the experiments. In the perturbative limit, one would, therefore, expect a minimum RMS energy fluctuation for the generated TH pulse to be $\mathrm{RMS_{TH}} = 3\mathrm{RMS_{NIR}} \cong 4.5\%$, represented by the dashed lines in Fig. 1c, which indeed corresponds to the measured value before the filament. But, inside the filament the RMS value is reduced to about 2.8%, which is significantly lower than the perturbative limit. This unequivocally demonstrates the stabilization of the TH pulse during the filamentation process. At the beginning of the filament, we observe an increase of the TH energy fluctuation which results from the fluctuation of the starting point of the filament for different initial peak power [16]. Beyond the filament the TH energy fluctuation increased as a function of the propagation distance since the TH generated inside the filament destructively interferes with the TH generated after the filament.

4 Numerical simulations

In order to reveal the physical reason for the self-stabilization of the TH energy, we used the theoretical model for the two-color filamentation in air described by the coupled equations given in (1)–(3) of [11]. The propagation equations include geometrical focusing, diffraction, group-velocity dispersion, self-focusing, plasma generation via multiphoton ionization and third-harmonic generation. For the numerical simulations we have considered the propagation of a linearly polarized, collimated Gaussian input laser pulse with a central wavelength at $\lambda_0 = 807$ nm which is focused with a 100 cm focal length lens in air at atmospheric pressure. We have used laser input powers, P_0, above the effective critical power, $P_{\mathrm{cr}} = \lambda_0^2/2\pi\, n_\omega\, n_2 = 8$ GW needed for self-focusing in air [17] and an initial beam radius of $w_0 = 2$ mm (at $1/e^2$ of intensity). In order to verify the stability of the TH pulse in the numerical simulations, we have performed a series of calculations, in which the initial pump parameters are varied according to the experimental conditions. The results presented below are an average of the numerical results for initial pump pulse duration, energy and peak power of 40 fs, 680 μJ and 16 GW, respectively, with a root-mean-square fluctuation of 1.5%.

In Fig. 1d we present the averaged TH energy along the propagation axis, the corresponding root-mean-square TH energy fluctuation is shown in Fig. 1e. The numerical simulations are in qualitative agreement with the experimental results. The conversion efficiency in both cases is about 0.1% inside the filament. From the numerical simulations we observe a RMS fluctuation of 1% for the TH energy at a position around 96 cm in Fig. 1e, while in the experiment a minimum RMS fluctuation of 2.8% has been observed inside the filament (cf. Fig. 1c). The difference in the TH energy distributions along the propagation axis originates from the elliptical beam profile used in the experiment while the numerical code was limited to a cylindrical symmetric beam profile. Thus, the larger beam diameter along the major axis of the elliptical beam profile would make the self-focus of the laser pulse closer to the geometrical focus and generates a shorter filament for the experiment. The higher value of the experimental RMS energy fluctuation as compared to the numerical results can result from two factors: 1) between the first wedge (W1) and the decoupling mirror (DM) in Fig. 1a there was no filament; thus, the laser intensity was not clamped. 2) The distance between the first wedge (W1) and the decoupling mirror (DM) corresponds to three times the coherence length ($\pi/\Delta k$). Thus, the destructive in-

terference of the TH pulse between the first wedge and the decoupling mirror would increase the fluctuation of the TH energy mainly because of the intensity fluctuation and the phase mismatch with the NIR pulse.

Since the TH pulse is generated by the pump, it is obvious to expect that the reason for the stabilization of the TH pulse inside the filament is due to a stabilization of the pump pulse itself. This correlation is indeed the case, as it can be seen from the comparison of the results for the mean intensity distributions of the NIR and TH pulses along the propagation axis, presented in Fig. 2a and b. The corresponding RMS intensity fluctuations are shown in Fig. 2c and d, where the initial RMS intensity fluctuation of the input NIR pulses of 1.5% is represented by the dashed line in Fig. 2c. As outlined above, in the perturbative limit, one would expect a minimum RMS intensity fluctuation for the third-harmonic pulse of 4.5%, which corresponds to the dashed lines in Fig. 2d.

It is clearly seen from the comparison that both the mean intensity distribution as well as the RMS intensity fluctuation of the TH pulse along the propagation follow closely the respective curves for the pump pulse. At the beginning of the filament ($z = 85$ cm), we observe an increase of the RMS intensity fluctuation for both the NIR and TH pulses due to the vacillations of the starting point of the filament for different initial pump pulse parameters in the numerical average [16]. Inside the filament (between 90 cm to 100 cm), for both pulses there is seen the steep decrease of the RMS intensity fluctuation below the initial (for the pump pulse) or the expected perturbative values (for the TH pulse). This is obviously due to the intensity clamping of the pump pulse inside the core of the filament. This stabilization of the laser intensity can be used for nonlinear intensity dependent processes during the two-color filamentation. Beyond the filament the RMS intensity fluctuation of the NIR pulse is higher than its initial value because the vacillation of the starting point of the filament provokes a fluctuation of the far-field NIR beam diameter. Thus, the NIR cross-section becomes unstable and increases the pump intensity fluctuation.

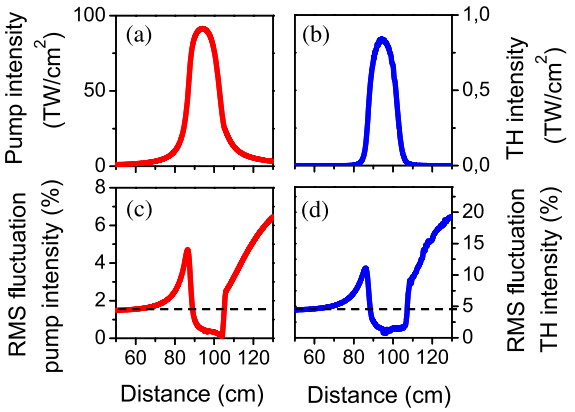

FIGURE 2 Longitudinal distribution of (**a**) the mean pump intensity and (**b**) the generated third-harmonic intensity. The respective root-mean-square (RMS) fluctuation is shown in (**c**) for the pump intensity and (**d**) for the third-harmonic intensity. The fluctuation of the initial peak power was RMS = 1.5%

Similarly, the TH intensity variation increases after the filament due to the rise of the NIR intensity fluctuation and the destructive interference with the third-harmonic generated beyond the filament.

The energy of the third-harmonic ($E_{3\omega}$) depends on the TH intensity ($I_{3\omega}$) distribution integrated in time and space, $E_{3\omega} = \iiint I_{3\omega}(r, \theta, \tau) r\,\mathrm{d}r\,\mathrm{d}\theta\,\mathrm{d}\tau \propto I_{3\omega}\varphi_{3\omega}^2\tau_{3\omega}$, where $\varphi_{3\omega}$ and $\tau_{3\omega}$ are the effective diameter and the effective pulse duration of the TH pulse inside the filament. Recently, it has been observed that the filament diameter is not constant when the initial peak power changes: the filament diameter increases as a function of the initial pump power because of the counterbalance between the laser energy confined by the external focusing and the defocusing effect of the plasma [18, 19]. On the other hand, as the pump power increases, the filament length increases;

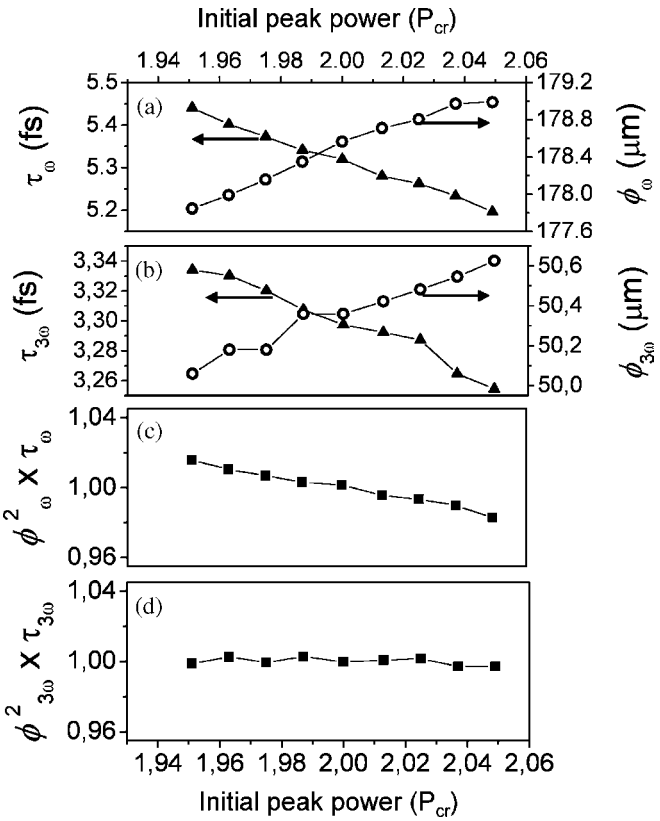

FIGURE 3 Numerical results of the pulse duration (τ) and the diameter (φ) inside the filament at $z = 96$ cm for (**a**) the pump pulse and (**b**) the third-harmonic pulse as a function of the initial pump peak power. The product $\varphi_\omega^2\tau_\omega$ (arb. units) for the fundamental pulse and the product $\varphi_{3\omega}^2\tau_{3\omega}$ (arb. units) for the third-harmonic pulse are shown in (**c**) and (**d**), respectively, as a function of the initial pump peak power

thus, the spectral broadening is more pronounced [20] and the pulse duration decreases [21]. Thus, if the filament diameter and the pulse duration are not stable when the initial pump power changes, there is one question which needs to be answered: how can the filamentation stabilize the energy of the generated third-harmonic pulse? For an initially fixed pulse duration, the results of simulations in Fig. 3 show that the pulse durations of both the NIR and TH pulses decrease as a function of the initial peak power while their beam diameters increase inside the filament. It is interesting to note parenthetically that the effective pulse duration of the TH pulse reaches about 3.3 fs inside the filament, which corresponds to 3–4 cycles. Thus, both the cross-section of the filament and the laser pulse duration are not stabilized during the filamentation as observed previously. However, as shown in Fig. 3, these parameters are anticorrelated and their product $\varphi_{\mathrm{eff}}^2\tau_{\mathrm{eff}}$, which corresponds in fact to the effective 'volume' of the laser pulse, is stable in Fig. 3c (for the pump pulse) and Fig. 3d (for the TH pulse) for small variations of the initial NIR peak power. It is important to note that the effective diameter and pulse duration of the fundamental pulse shown in Fig. 3a are affected by the noisy energy reservoir surrounding the filament core. On the order hand, the third-harmonic pulse is generated inside the constant (clamped) high intensity zone of the filament core. Thus, the effective diameter and pulse duration of the third-harmonic pulse, shown in Fig. 3b, are not affected by this noisy energy reservoir. The RMS fluctuation of the product $\varphi_{3\omega}^2\tau_{3\omega}$ is 0.2% and, hence, lower than the corresponding value of 0.9% in case of the pump pulse. Thus, the stabilization of the third-harmonic energy observed both theoretically and experimentally results from the intensity clamping and the stabilization of laser pulse 'volume' inside the filament.

We may finally note that the self-stabilization during filamentation can also be observed by the plasma generation. The ionization of N_2 requires the absorption of 10 photons at a wavelength of 807 nm. The measured RMS fluctuation of the N_2^+ fluorescence strength was 8% inside the filament, which is two times more stable than the fluorescence fluctuation $\mathrm{RMS}_{N_2} = 10\mathrm{RMS}_{\mathrm{NIR}} = 15\%$ expected from a perturbative estimation for an initial fluctuation of 1.5% of the pump intensity. This stabilization of the N_2^+ fluorescence is also the result of the intensity clamping and the constant laser 'volume' inside the filament.

5 Conclusion

In conclusion, we have demonstrated both numerically and experimentally the stabilization of the high-intensity filament core, the third-harmonic energy and the self-generated plasma density. These stabilizations are the results of intensity clamping of the pump pulse and a constant 'volume' of the laser pulse due to the dynamic equilibrium between the nonlinear intensity dependent Kerr effect and the defocusing effect of the low density plasma. Nevertheless, from the statistical analysis of numerical simulations we observe that the pulse duration fluctuation is not improved during the filamentation and becomes slightly higher than its initial value.

ACKNOWLEDGEMENTS This work was supported by Natural Sciences and Engineering Research Council of Canada (NSERC), Defence R&D Canada – Valcartier (DRDC – Valcartier), Le Fonds Québécois de la Recherche sur la Nature et les Technologies (FQRNT), Canada Research Chairs (CRC), Canada Foundation for Innovation (CFI) and Canadian Institute for Photonic Innovations (CIPI). The authors appreciate the technical support of Mr. Mario Martin.

REFERENCES

1 A.H. Zewail, J. Phys. Chem. **100**, 12 701 (1996)
2 M. Hentschel, R. Kienberger, C. Spielmann, G.A. Reider, N. Milosevic, T. Brabec, P. Corkum, U. Heinzmann, M. Drescher, F. Krausz, Nature **414**, 509 (2001)
3 C.P. Hauri, W. Kornelis, F.W. Helbing, A. Heinrich, A. Couairon, A. Mysyrowicz, J. Biegert, U. Keller, Appl. Phys. B **79**, 673 (2004)
4 A. Couairon, M. Franco, A. Mysyrowicz, J. Biegert, U. Keller, Opt. Lett. **30**, 2657 (2005)
5 A. Guandalini, P. Eckle, M. Anscombe, P. Schlup, J. Biegert, U. Keller, J. Phys. B **39**, S257 (2006)
6 S.L. Chin, S.A. Hosseini, W. Liu, Q. Luo, F. Théberge, N. Aközbek, A. Becker, V.P. Kandidov, O.G. Kosareva, H. Schroeder, Can. J. Phys. **83**, 863 (2005)
7 J. Kasparian, R. Sauerbrey, S.L. Chin, Appl. Phys. B **71**, 877 (2000)
8 A. Becker, N. Aközbek, K. Vijayalakshmi, E. Oral, C.M. Bowden, S.L. Chin, Appl. Phys. B **73**, 287 (2001)
9 M. Mlejnek, E.M. Wright, J.V. Moloney, Opt. Lett. **23**, 382 (1998)
10 F. Théberge, N. Aközbek, W.W. Liu, A. Becker, S.L. Chin, Phys. Rev. Lett. **97**, 023 904 (2006)
11 N. Aközbek, A. Iwasaki, A. Becker, M. Scalora, S.L. Chin, C.M. Bowden, Phys. Rev. Lett. **89**, 143 901 (2002)
12 M. Kolesik, E.M. Wright, A. Becker, J.V. Moloney, Appl. Phys. B **85**, 531 (2006)
13 N. Kortsalioudakis, M. Tatarakis, N. Vakakis, S.D. Moustaizis, M. Franco, B. Prade, A. Mysyrowicz, N.A. Papadogiannis, A. Couairon, S. Tzortzakis, Appl. Phys. B **80**, 211 (2005)
14 J.R. Sutherland, E.L. Christensen, N.D. Powers, S.E. Rhynard, J.C. Painter, J. Peatross, Opt. Express **12**, 4430 (2004)
15 R.W. Boyd, J. Opt. Soc. Am. **70**, 877 (1980)
16 A. Brodeur, S.L. Chin, J. Opt. Soc. Am. B **16**, 637 (1999)
17 W. Liu, S.L. Chin, Opt. Express **13**, 5750 (2005)
18 Y.P. Deng, J.B. Zhu, Z.G. Ji, J.S. Liu, B. Shuai, R.X. Li, Z.Z. Xu, F. Théberge, S.L. Chin, Opt. Lett. **31**, 546 (2006)
19 F. Théberge, W. Liu, P.T. Simard, A. Becker, S.L. Chin, Phys. Rev. E **74**, 036 406 (2006)
20 F. Théberge, W. Liu, S.A. Hosseini, Q. Luo, S.M. Sharifi, S.L. Chin, Appl. Phys. B **81**, 131 (2005)
21 J. Liu, X.W. Chen, J.S. Liu, Y. Zhu, Y.X. Leng, J. Dai, R.X. Li, Z.Z. Xu, Opt. Express **14**, 979 (2006)